CELL CYCLE
2019, VOL. 18, NO. 4, 395–412
https://doi.org/10.1080/15384101.2018.1564492

Taylor & Francis
Taylor & Francis Group

RESEARCH PAPER

PKCβ1 regulates meiotic cell cycle in mouse oocyte

Zi-Yun Yi[a], Qiu-Xia Liang[a], Tie-Gang Meng[b], Jian Li[a], Ming-Zhe Dong[b], Yi Hou[b], Ying-Chun Ouyang[b], Chun-Hui Zhang[a], Heide Schatten[c], Qing-Yuan Sun[b], Jie Qiao[d], and Wei-Ping Qian[a]

[a]The Reproductive Medicine Center, Peking University Shenzhen Hospital, Shenzhen Peking University-The Hong Kong University of Science and Technology Medical Center, Shenzhen, China; [b]State Key Laboratory of Stem Cell and Reproductive Biology, Institute of Zoology, Chinese Academy of Sciences, Beijing, China; [c]Department of Veterinary Pathobiology, University of Missouri-Columbia, Columbia, MO, USA; [d]Reproductive Medical Center, Peking University Third Hospital, Beijing, China

ABSTRACT

PKCβI, a member of the classical protein kinase C family, plays key roles in regulating cell cycle transition. Here, we report the expression, localization and functions of PKCβI in mouse oocyte meiotic maturation. PKCβI and p-PKCβI (phosphor-PKCβI) were expressed from germinal vesicle (GV) stage to metaphase II (MII) stage. Confocal microscopy revealed that PKCβI was localized in the GV and evenly distributed in the cytoplasm after GV breakdown (GVBD), and it was concentrated at the midbody at telophase in meiotic oocytes. While, p-PKCβI was concentrated at the spindle poles at the metaphase stages and associated with midbody at telophase. Depletion of PKCβI by specific siRNA injection resulted in defective spindles, accompanied with spindle assembly checkpoint activation, metaphase I arrest and failure of first polar body (PB1) extrusion. Live cell imaging analysis also revealed that knockdown of PKCβI resulted in abnormal spindles, misaligned chromosomes, and meiotic arrest of oocytes arrest at the Pro-MI/MI stage. PKCβI depletion did not affect the G2/M transition, but its overexpression delayed the G2/M transition through regulating Cyclin B1 level and Cdc2 activity. Our findings reveal that PKCβI is a critical regulator of meiotic cell cycle progression in oocytes.

Abbreviations: PKC, protein kinase C; COC, cumulus-oocyte complexes; GV, germinal vesicle; GVBD, germinal vesicle breakdown; Pro-MI, first pro-metaphase; MI, first metaphase; Tel I, telophase I; MII, second metaphase; PB1, first polar body; SAC, spindle assembly checkpoint

KEYWORDS

PKCβ1; oocyte; meiosis; germinal vesicle breakdown; spindle

Introduction

Mouse oocyte maturation is a multi-stage, precisely orchestrated process [1,2] . Resumption of oocyte maturation is characterized by germinal vesicle breakdown (GVBD), followed by microtubule assembly around chromosomes, and formation of a bipolar meiotic spindle. Then, the oocyte undergoes metaphase I (MI), emits the first polar body, and enters into metaphase II (MII) with the spindle located beneath the plasma membrane [3]. Subsequently, the oocyte arrests at the MII stage until fertilization takes place [4,5]. Pivotal stages for regulation of oocyte meiotic maturation in mammals are the prophase I arrest and progression from MI to MII [5].

Prophase I arrest, also termed the germinal vesicle (GV) stage, is closely associated with low maturation promoting factor (MPF) activity [6]. MPF is a complex of a central cell cycle regulator in all eukaryotic cells, composed of a catalytic subunit $p34^{cdc2}$ kinase (CDK1; also known as Cdc2) and regulatory subunit cyclin B1 [7]. MPF remains inactive until Cdk1 is phosphorylated at Thr161 by Cdk activating kinase (CAK) and dephosphorylated by Cdc25 at Thr14/Tyr15 [8,9]. The cyclin-dependent kinase inhibitor p21 contributes to cell cycle arrest in G2 by blocking the activating phosphorylation of Cdc2 on Thr161 [10]. Wee1 and Myt1 protein kinases phosphorylate and inhibit CDK1 activity, whereas the cell division cycle 25B (Cdc25B), a substrate of PKA, can release CDK1 activity by dephosphorylating Wee1B-phosphorylated CDK1 [11,12]. During prophase arrest, anaphase-promoting complex/cyclosome (APC/C) is responsible for Cyclin B 1 destruction and inactivation of MPF [13]. In GV stage oocytes, Cdh1 is required for APC/C -mediated cyclin B1 destruction to arrest at prophase I [13]. Accumulation of cyclin B1 and activation of MPF in GV oocytes leads to GVBD (G2/M transition) [14]. While during MI to MII

CONTACT Wei-Ping Qian qianweipingsz@126.com

transition, MPF activity decreases transiently, as cyclin B1 is continuously degraded in a ubiquitin-dependent manner [15]. Many other proteins, such as phosphodiesterase 3A (PDE3A), protein kinase A, protein kinase C, Aurora kinase A, Polo-like kinase 1 (plk1), BubR1, calcium/calmodulin-dependent protein kinase II (CaMKII) and mitogen-activated protein kinase (MAPK) have been reported to regulate the resumption of meiosis in mammalian oocytes [16–19].

Protein kinase C (PKC) is a multi-gene family of serine/threonine kinases that have been reported to regulate cell-cycle transitions in somatic cells [20]. The PKC family consists of 11 different isotypes subdivided into classical PKCs (c PKC -α, -βI,-βII,-γ), novel PKCs (n PKC -δ, -ε, -η, -θ, -μ) and atypical PKCs (a PKC-λ/τ, -ζ) based on their structure domain and activation [20–22]. It has been shown that PKC isoforms (PKC-α, -βI, -βII, -γ, -δ, -λ, -ζ, -μ) are expressed in mouse oocytes [23]. Mounting evidence indicates that PKC is a key regulator of critical cell cycle transition during mitosis, including G1/S and G2/M, affecting different molecules including cyclins, cyclin-dependent kinases (Cdk), Cip/Kip inhibitors and lamins [24–26].

PKCs also appear to have multiple functional roles in the cell cycle progression during oocyte meiotic maturation [27]. Activation of PKC is a sufficient and necessary event to block spontaneous germinal vesicle breakdown (GVBD) in denuded oocytes [28–30], but it induces meiosis resumption in cumulus cell-enclosed oocytes (CEOs) through the mediation of cumulus cells [31,32]. Our previous study showed that PKC activators inhibited GVBD in denuded mouse oocytes by preventing the phosphorylation of MAPK [33,34]. Activation of PKC with TPA arrests mouse oocytes at the MI stage and blocks polar body emission [23], while suppression of PKC with its inhibitor BIM promotes the onset of anaphase I in a dose-dependent manner [35,36]. Phospho-PKC was distributed to the meiotic spindle, while it was concentrated at the midbody in telophase during mouse oocytes meiosis, which suggested that PKC activation might play important roles in regulating spindle organization and stabilization [35]. PKC-mediated regulation of these transitions may be either negative or positive, depending on the timing of PKC activation during the cell cycle and the specific PKC isoforms involved [37]. Up to date, the functions of PKC during mouse oocyte meiotic maturation were mainly studied by various PKC inhibitors and activators, which are not selective for a particular type of enzyme. While, as the research further develops, illustration of the role of the PKC subtypes in meiotic maturation is necessary.

PKCβ1 is one of the classical PKC isoforms and its function in meiotic maturation is still far from clear. It has been shown that PKCβ1 was present in the cytoplasm at the start of the process and migrated to the nucleus/germinal vesicle before GVBD [38], but it evenly distributed in the cytoplasm and in the plasma membrane at the metaphase II (MII) stages [29,33]. HX alone maintained PKCβ1 in the cytoplasm, whereas FSH and PKC activation partly induced its translocation into the nucleus [31]. It was reported that cytoplasmic PKCβ1 leads to maintenance of meiotic arrest, but nuclear PKCβ1 may be involved in the resumption of meiosis [38]. FSH-induced inactivation of PKCβI in granulosa cells participates in mouse oocyte meiotic resumption, possibly by activation of the EGFR signaling pathway [39]. Moreover, in preliminary results, PKCβ1 colocalized with lamin A/C on the nuclear envelope in mouse oocytes and it plays a role in the phosphorylation of lamins that accompanies the mitotic nuclear breakdown at the G2/M transition [38,40].

It has been reported that T cell polarization and locomotion is associated with translocation of PKCβ1 to the microtubule cytoskeleton [41]. In human leukemia cells, PKCβ1 has been shown to colocalize with microtubules and bind microtubule-associated proteins [42]. Polar body emission requires a classical RhoA contractile ring and Cdc42-mediated membrane protrusion [43]. Specially, Cdc42 and Rho activity are enhanced by PKCβ in Xenopus oocytes [44].

Here, we for the first time investigated the functions of PKCβ1 during mouse oocyte meiotic maturation by using RNA interference (RNAi) and overexpression approaches. Our results revealed that depletion of PKCβ1 arrested oocytes at the Pro-MI/MI stage and caused failure of first polar body extrusion by affecting spindle organization during mouse oocyte meiotic maturation.

Furthermore, we showed that overexpression of PKCβ1 inhibited meiotic resumption by causing decreased cyclin B1 level and Cdc2 activity.

Results

PKCB1 expression and subcellular localization during mouse oocyte meiotic maturation

The PKCβ1 m RNA level was detected by quantitative RT-PCR. PKCβ1 mRNA expression was detected at the GV, MI and MII stages. The PKCβ1 mRNA levels at the MI and MII stages were 57.16 ± 6.72% and 35.64 ± 7.76% of that of the GV stage (Figure 1(a)). We cultured oocytes for 0h, 4h, 8h and 12h, corresponding to germinal vesicle (GV), pro-metaphase I (Pro-MI), metaphase I (MI) and metaphase II (MII) stages, respectively. Western blotting results showed that the expression level of PKCβ1 was stable from GV to MI stages, and then increased slightly at MII (Figure 1(b)). To validate the subcellular specific distribution of PKCβ1 during meiotic maturation, immunofluorescent staining was performed using a PKCβ1 antibody. As shown in Figure 1(c), PKCβ1 was concentrated in the entire germinal vesicle except for the nucleolus, with a weak expression in the cytoplasm. At GVBD, MI and MII stages, PKCβ1 mainly evenly distributed in the cytoplasm and in the plasma membrane as well, while it was located at the midbody at the Tel I stage.

To further investigate the subcellular localization of PKCβ1 during meiotic maturation, we injected Myc-PKCβ1 mRNA into oocytes at the GV stage. The control group was injected with the same amount of Myc-mRNA. After microinjection of PKCβ1-myc mRNA(2.5mg/ml) or Myc mRNA, oocytes were incubated in M2 medium containing 200μm IBMX for

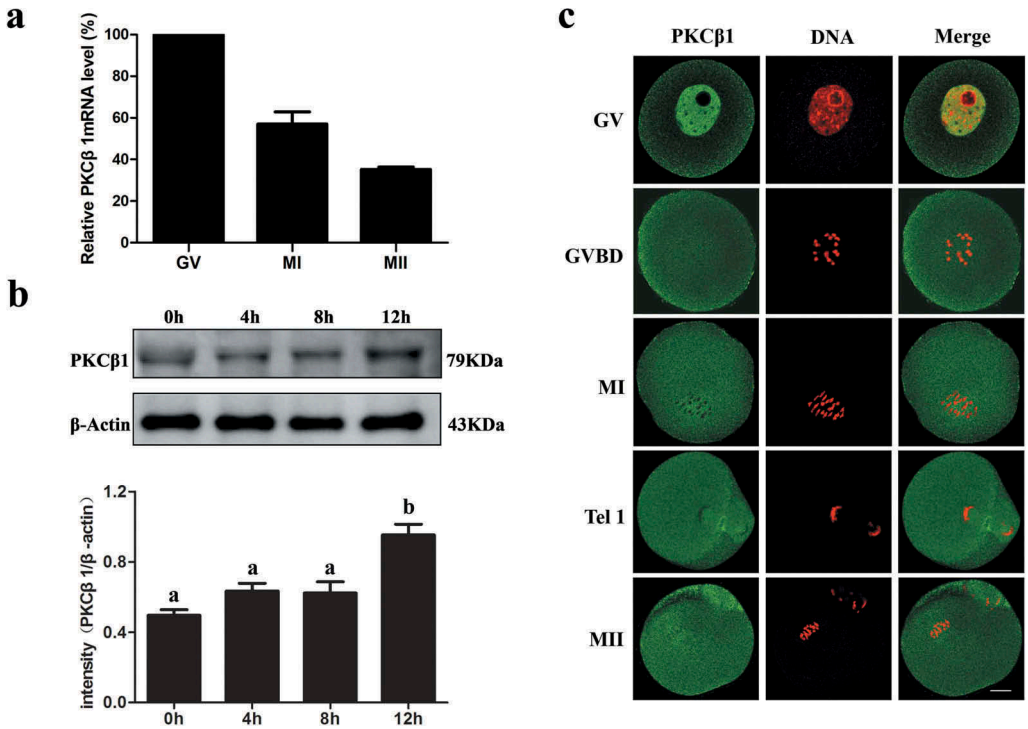

Figure 1. Expression and subcellular localization of PKCβ1 during mouse oocyte meiotic maturation. (a) Relative level of PKCβ1 mRNA meiotic maturation. Samples were collected for quantitative RT-PCR after oocytes were cultured for 0h, 8h or 12h, representing GV, MI or MII stages, respectively. PKCβ1 mRNA levels were normalized to the maximum levels at the GV stage. Each sample contains 50 oocytes. (b) Protein level of PKCβ1 identified by Western blotting. Oocytes were collected for 0h, 4h, 8 h or 12h, corresponding to GV, GVBD, MI or MII stages. Each sample contained 200 oocytes. The intensity of PKCβ1/β-actin was accessed by grey level analysis. The molecular mass of PKCβ1 and β-actin were 79kDa and 43kDa, respectively. Data are expressed as mean ± SEM and different letters indicate statistically significant difference ($p < 0.05$). (c) Subcellular localization of PKCβ1 shown by confocal microscopy in mouse oocytes at GV, GVBD, MI, Tel I and MII stages. Green, PKCβ1; red, chromatin; each sample was counterstained with Hoechst 33,342 to visualize DNA (red). Bar = 20μm.

12h, and then collected for Western blot analysis with anti-myc antibody. As shown in Figure 2(a), Western blotting showed a high level of PKCβ1 protein expression in the myc-PKCβ1 mRNA injected group, while no specific blot was detected in the control group. To further examine Myc-PKCβ1 localization in meiotic maturation, we injected a low concentration of PKCβ1-myc mRNA (about 0.4mg/ml, 5–10 pl/oocyte) into oocytes. Myc-fluorescein isothiocyanate (FITC) monoclonal antibody was used to detect the localization of Myc- PKCβ1. At the GV stage, Myc-PKCβ1 mainly concentrated in the germinal vesicle. From the GVBD to MII stages, it mainly distributed in the cytoplasm. At Tel I, it was located at the mid-body (Figure2(c)).

Next we microinjected myc mRNA (about 0.4mg/ml) into the GV stage oocytes. Myc-fluorescein isothiocyanate (FITC) monoclonal antibody was used to verified the distribution of Myc. From the GV to MII stages, Myc distributed dispersedly in mouse oocytes (Figure 2(d)).

Expression and subcellular localization of p-PKCβ1 during mouse oocyte meiotic maturation

Since phosphorylation of PKCβ1 is very critical in controlling the catalytic activity, stability and intracellular localization of PKCβ1, we examined the expression and subcellular localization of

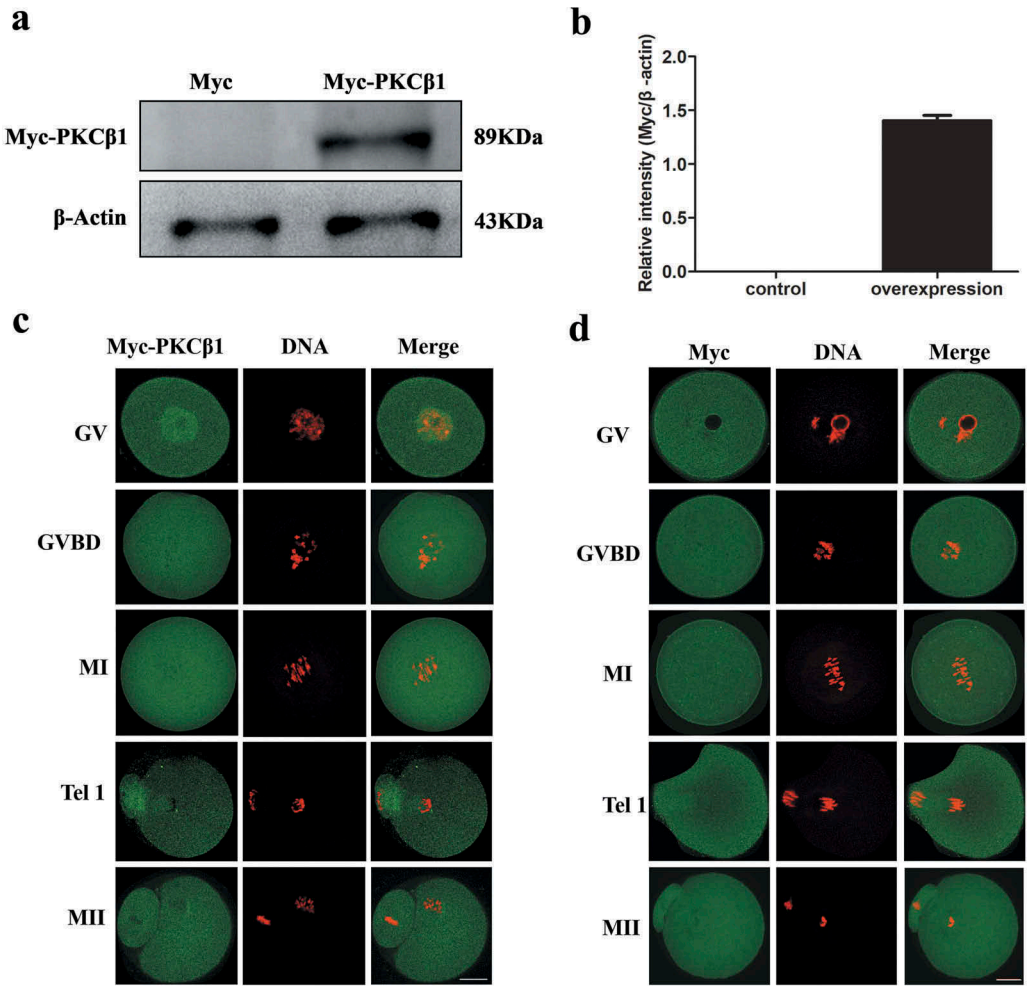

Figure 2. Expression and subcellular localization of Myc-PKCβ1 during mouse oocyte meiotic maturation. (a) Myc-PKCβ1 expression in oocytes injected with Myc-PKCβ1 mRNA. Myc mRNA and Myc-PKCβ1 mRNA injected oocytes were collected for Western blot analysis. After microinjection of PKCβ1-myc mRNA (2.5mg/ml) or Myc mRNA, oocytes were incubated in M2 medium containing 200μm IBMX for 12h, and then collected for Western blot analysis. Each sample contains 200 oocytes. (b) The intensity of Myc-PKCβ1/β-actin was accessed by grey level analysis. The molecular mass of Myc-PKCβ1 was 89 kDa. (c) Myc-PKCβ1 mRNA-injected oocytes at GV, GVBD, MI, TI and MII stages were stained with anti-Myc antibody. Green, Myc-PKCβ1; red, chromatin; each sample was counterstained with Hoechst 33,342 to visualize DNA (red). Bar = 20μm. (d) Confocal microscopy of showing the subcellular localization of Myc (green) in myc mRNA-injected oocytes at GV, GVBD, MI, T1 and MII stages. Green, Myc; red, chromatin. Bar = 20μm.

p-PKCβ1 during meiotic maturation. We cultured oocytes for 0h, 4h, 8h, 12h, corresponding to GV, GVBD, MI and MII stages, respectively. The Western blotting showed that the p-PKCβ1 protein was expressed from GV to MII stages without detectable change (Figure 3(a-b)).

To investigate the subcellular localization of p-PKCβ1 during meiotic maturation, mouse oocytes were cultured and processed for immunofluorescent staining at different stages. As shown in Figure 3(c), p-PKCβ1 was mainly distributed in germinal vesicle at the GV stage. After GVBD, p-PKCβ1 gradually accumulated in the vicinity of condensed chromosomes. At pro-MI stage, p-PKCβ1 migrated to the spindle poles before the chromosomes congressed at the equator of the spindle. In metaphase, p-PKCβ1 was found to accumulate at spindle poles. At the stage of anaphase I, p-PKCβ1 was localized at the midbody and accumulated in the vicinity of chromosomes.

PKCβ1 depletion does not affect GVBD, but causes abnormal spindles, Pro-MI/MI arrest and reduced PB1 extrusion

To dissect the roles of PKCβ1 during mouse oocyte meiotic maturation, PKCβ1 specific siRNA was used to perturb the function of PKCβ1. Both Western blotting analysis and immunostaining showed that the expression level of PKCβ1 was notably reduced (Figure 4(a-b)), which revealed the efficiency of PKCβ1 depletion. What's more, Western blotting showed that the expression level of p-PKCβ1 was notably reduced after PKCβ1 specific siRNA injection (Figure 4(a)). After PKCβ1 specific or control siRNA injection, the oocytes were cultured in M2 medium containing 200μM IBMX. Then, the oocytes were continuously cultured in IBMX-free M2 medium for 4h or 14h. In the PKCβ1 depletion group, oocytes exhibited morphologically defective spindles (Figure 4(c)). Chromosome misalignment was also observed (Figure 4(c)). The major spindle defects were spindle with no pole, one pole, others were multi-pole spindle,

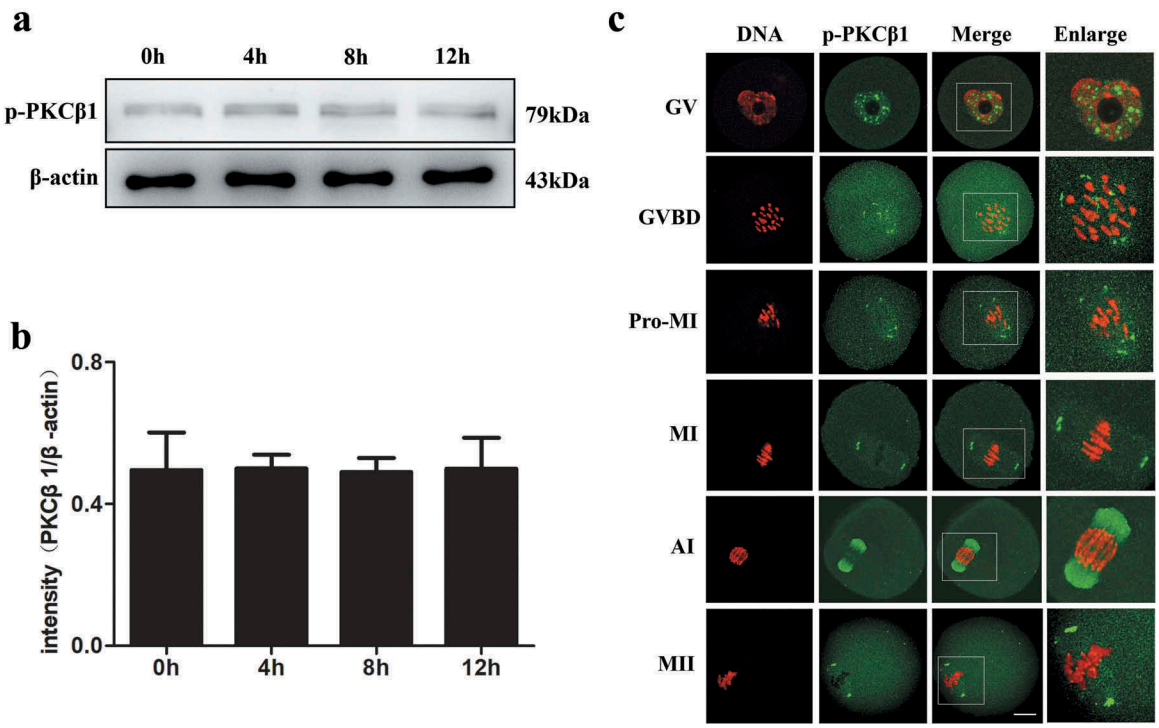

Figure 3. Expression and subcellular location of p-PKCβ1 during oocyte meiotic maturation. (a)Expression of p-PKCβ1 protein identified by Western blotting. Samples of 200 oocytes were collected after culture of 0, 4, 8 and 12 h, corresponding to GV, GVBD, MI and MII stages, respectively. The molecular mass of p-PKCβ1 and β-actin were 79kDa and 43kDa, respectively. Each sample contained 200 oocytes. (b)The intensity of p-PKCβ1/β-actin was accessed by grey level analysis. (c) Confocal microscopy showing the subcellular localization of p-PKCβ1 at GV, GVBD, Pro-MI, MI, AI and MII stages. Green, PKCβ1; red, chromatin; each sample was counterstained with Hoechst 33,342 to visualize DNA (red). Magnifications of the boxed regions are shown on the right of each main panel. Bar = 20μm.

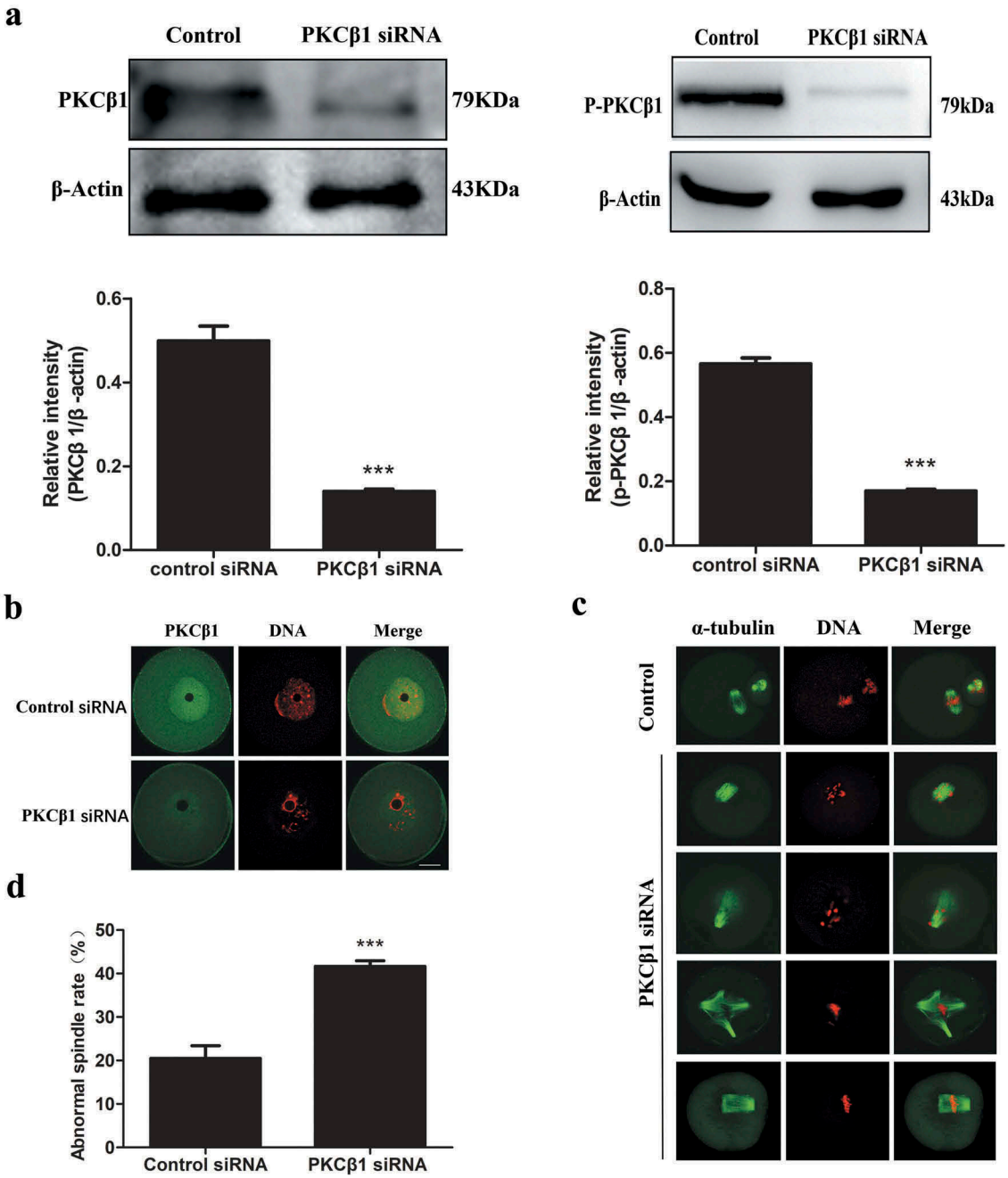

Figure 4. Depletion of PKCβ1 causes severely abnormal spindle and misaligned chromosomes in oocytes. After microinjection of PKCβ1 siRNA or control siRNA, the oocytes were incubated in M2 medium containing 200μM IBMX for 24h, then washed 3 times and transferred to IBMX-free M2 medium. (a) Western blotting of PKCβ1 and p-PKCβ1 in the PKCβ1 siRNA group and control group. After 24h inhibition in 200μm IBMX, the oocytes were collected for Western blotting. The intensity of PKCβ1/β-actin and p-PKCβ1/β-actin were accessed by grey level analysis. The molecular mass of PKCβ1 is 79kDa, the molecular mass of p-PKCβ1 is 79kDa and that of β-actin is 43kDa. Each sample contained 200 oocytes. (***$p < 0.001$) (b) Confocal microscopy showing depletion of PKCβ1 protein after siRNA injection. After 24 h inhibition in 200μm IBMX. A total of 56 oocytes were assessed in the PKCβ1 siRNA-group and 60 oocytes were assessed in the control siRNA-group. Green, PKCβ1; red, chromatin. Bar = 20μm. (c) Oocytes microinjected with PKCβ1 or control siRNA were incubated in M2 medium containing 200μm IBMX for 24h, and then transferred to IBMX-free M2 for 14h, followed by staining of α-tubulin (green) and DNA (red) to visualize spindles and chromosomes. In the PKCβ1 siRNA injection group, the oocytes exhibited various morphologically abnormal spindles and misaligned chromosomes. Bar = 20μm. (d) Percentage of oocytes with abnormal spindles in the PKCβ1-depletion group and control group. Data are presented as means± SEM of 3 independent experiments (*** $p < 0.001$).

broad spindle or displayed malformed spindles with astral microtubules (Figure 4(c)). The proportion of abnormal spindles in the PKCβ1-knockout oocytes (41.66 ± 1.29%,n = 157) was significantly higher than that in the control group (20.50 ± 2.90%, n = 171) (p<0.001, Figure 4(d)).

After microinjection of PKCβ1 siRNA or control siRNA, oocytes were placed in M2 medium containing 200μM IBMX for 24h. The oocytes were then continuously cultured in fresh IBMX-free M2 medium for 10h. As shown in Figure 5(a), the majority of PKCβ1-depleted oocytes were arrested at the Pro-MI /MI stage, with abnormal spindles, while most oocytes injected with control siRNA reached the anaphase I stage (Figure 5(a)). As shown in Figure 5(b), the Pro-MI/MI arrest in the PKCβ1 siRNA injected group (67.37 ± 4.21%, n = 64) was considerably higher than that in the control siRNA injected group (33.33 ± 2.57%, n = 57).

After microinjection of PKCβ1 siRNA or control siRNA, oocytes were placed in M2 medium containing 200μM IBMX for 24h and then continuously cultured in fresh IBMX-free M2 medium for 14h. As shown in Figure 5(c), the GVBD rate in the PKCβ1-knockdown group was similar to that in the control group. However, the first polar body (PB1) extrusion rate (48.59 ± 4.47%, n = 157) in the PKCβ1-knockdown group was significantly lower than that in the control group (80.94 ± 5.58%, n = 171). To confirm that PKCβ1-depleted oocytes were arrested at the Pro-MI/MI stage, we conducted chromosome-spreading experiments. Oocytes in both the PKCβ1 depletion group and the control group were cultured in IBMX-free M2 medium for 14h. Our results showed that chromosomes of the PKCβ1 depletion oocytes without PB1 were still in the bivalent state; in contrast, univalent chromosomes were observed in the control oocytes, indicating the

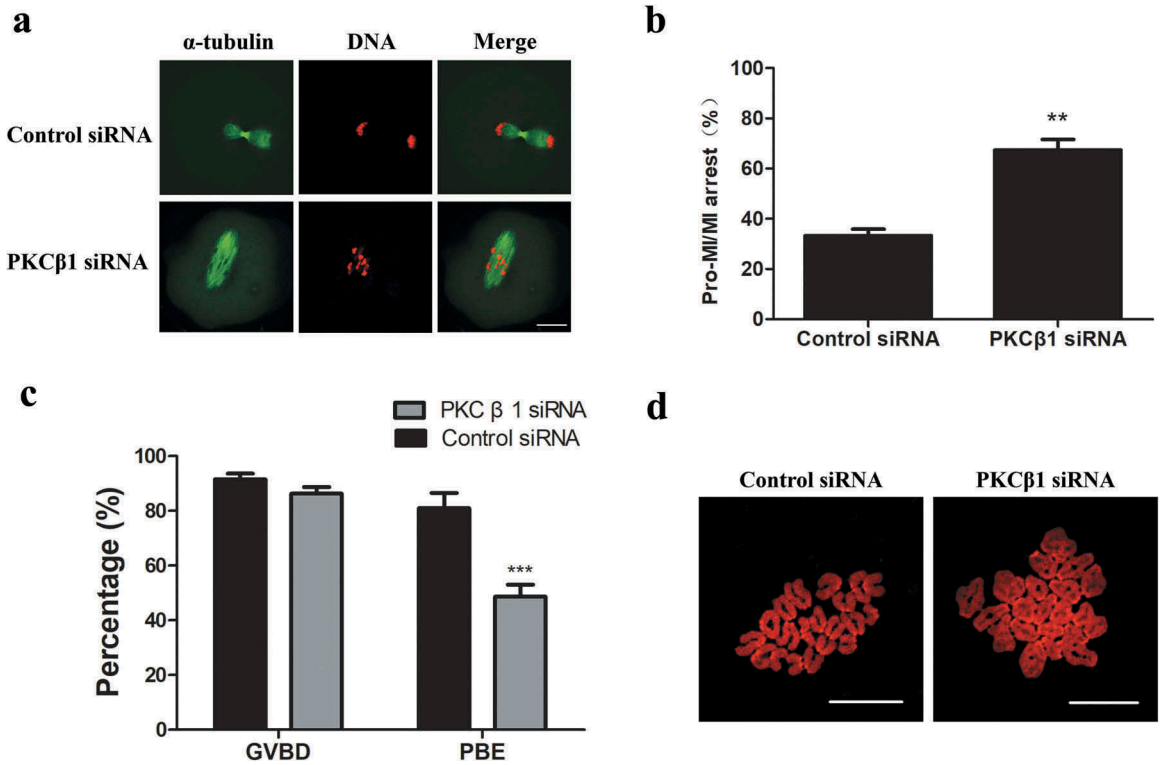

Figure 5. PKCβ1 depletion arrested oocytes at the Pro-MI/MI stage and caused failure of PB1 extrusion. After microinjection of PKCβ1 siRNA or control siRNA, the oocytes were placed in M2 containing 200μm IBMX for 24h, then transferred to IBMX-free fresh M2 medium for 10h or 14h. (a)Oocytes cultured for 10h in the PKCβ1 depletion group were arrested at the Pro-MI/MI stage, but oocytes in the control group had entered anaphase. Green, α-tubulin; red, chromatin. Bar = 20μm. (b) Percentage of Pro-MI/MI oocytes at 10h of culture in PKCβ1-delpletion group and control group. Data are presented as means± SEM of 3 independent experiments. (** $p < 0.01$). (c) Percentage of GVBD and PBE in the PKCβ1 siRNA group and control group. After microinjection of PKCβ1 siRNA or control siRNA, oocytes were incubated in M2 medium containing 200μm IBMX for 24h, then transferred to IBMX-free M2 medium after washing 3 times. GVBD rates were observed after 4h of maturation. Percentage of PBE was observed after 14h of culture. Data are presented as means ± SEM of 3 independent experiments. (*** $p < 0.001$). (d) Oocytes of the control and PKCβ1 depletion group were cultured for 14h, followed by chromosome spreading experiments.

completion of homologous chromosome separation (Figure5(d)).

PKCβ1 depletion causes activation of the SAC protein

Next, to further confirm the reason for the Pro-MI /MI arrest in PKCβ1 depleted oocytes, we analyzed the location of SAC protein Bub3 and Mad1 in oocytes. After 10h of culture, specific signals for Bub3 and Mad1 were detected on chromosome kinetochores in PKCβ1 knockdown oocytes, which were arrested at the Pro-MI/MI stage. In contrast, the control oocytes entered anaphase, without detection of Bub3 and Mad1 (Figure 6).

PKCβ1 knockdown prevents chromosome segregation and disturbs the metaphase-anaphase transition as revealed by time-lapse live imaging

Live-cell imaging showed that, in the control group, the meiotic spindle was visible and slowly migrated toward the oocyte cortex; then, a clear anaphase/telophase stage was observed, followed by rapid first polar body extrusion (Figure 7(a) and Video A). In contrast, in the PKCβ1 siRNA injected group, we found various morphologically abnormal spindles. Chromosomes failed to separate and oocytes remained at the Pro-MI/MI stage until about 14.5h after GVBD. In addition, no first polar body extrusion was observed (Figure 7(b) and Video B).

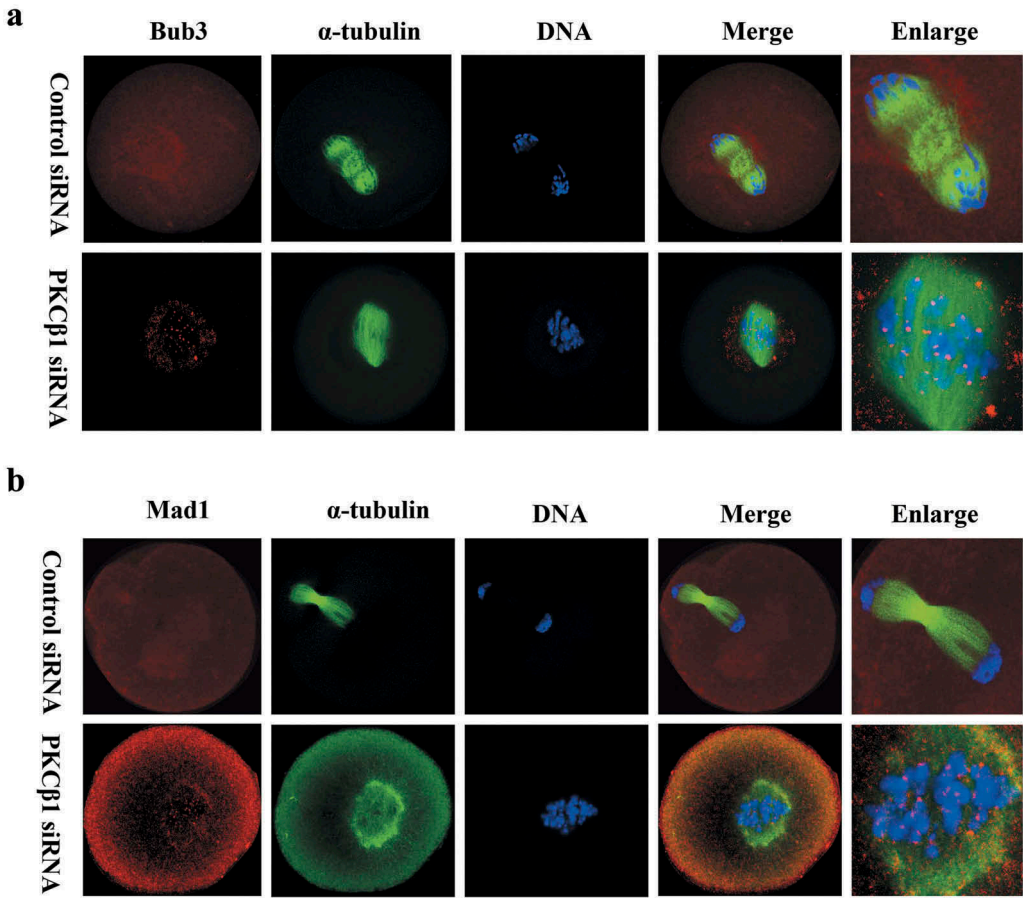

Figure 6. PKCβ1 depletion caused activation of SAC. Oocytes were arrested in M2 medium containing 200μm IBMX for 24h, following injection of PKCβ1 siRNA or control siRNA, then washed and cultured in IBMX-free M2 medium for10h. (a) Bub3 as marker of SAC was detected at the kinetochores in the PKCβ1-depletion group. Red, Bub3; green, α-tubulin; blue, DNA. Bar = 20μm. (b) Mad1 staining was used to further confirm the phenotype. Red, Mad1; green, α-tubulin; blue, DNA. Bar = 20μm.

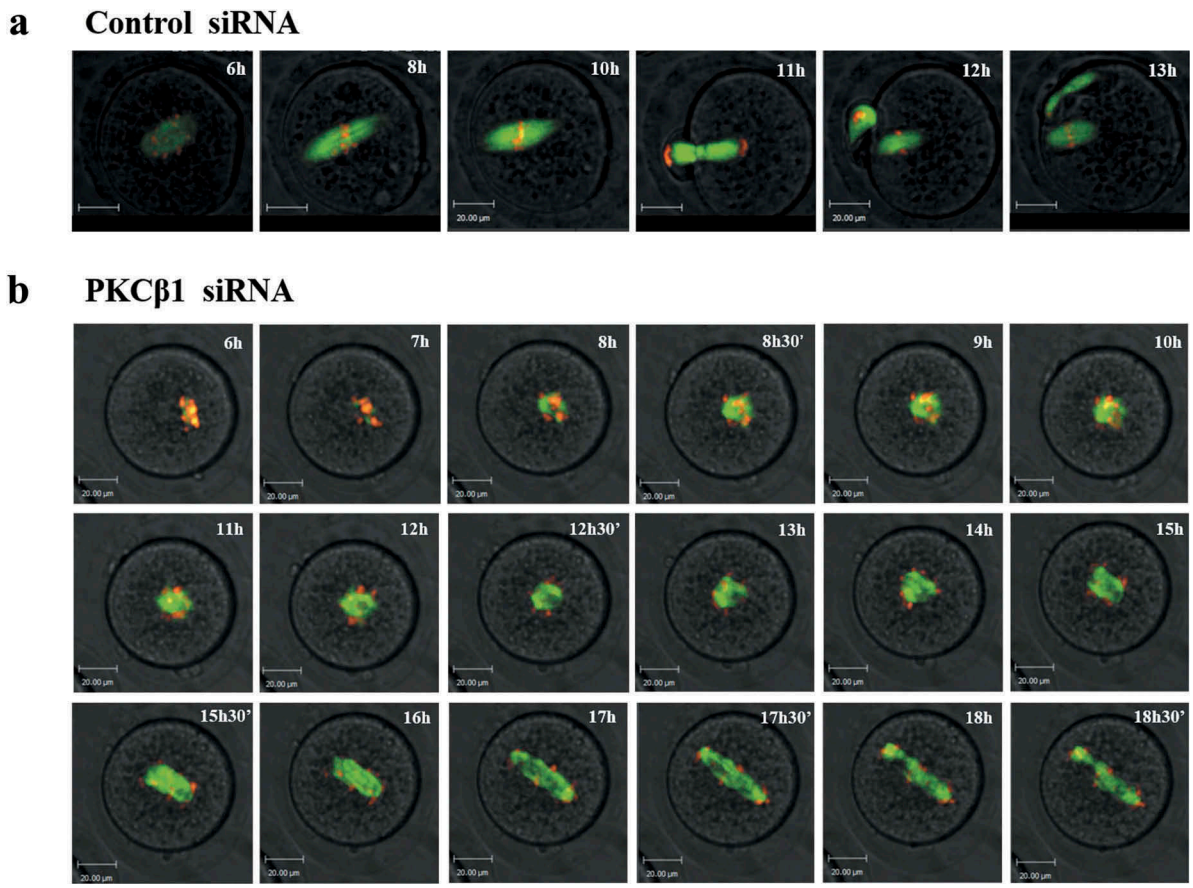

Figure 7. PKCβ1 knockdown disrupted the metaphase-anaphase transition of mouse oocytes as revealed by time-lapse live cell imaging. (a)Oocytes were co-injected with β5-tubulin-GFP mRNA, H2B-RFP mRNA and control siRNA. Spindle (fluorescent tubulin) and DNA (red) images in a representative control oocyte during in vitro maturation. Time points indicating the time lapse from GVBD occurrence in the oocytes. (b)Similar to (A), oocytes were co-injected with β5-tubulin-GFP mRNA, H2B-RFP mRNA and PKCβ1 siRNA. Representative images showing the PKCβ1 depleted oocytes with abnormal spindles, Pro-MI/MI arrested chromosomes, misaligned chromosomes, repetitive and unsuccessful chromosome segregation and PB1 extrusion failure. Green, tubulin; red, DNA. Bar = 20μm.

Exogenous overexpression of PKCβ1 delays oocyte meiotic resumption by regulating Cyclin B1, CyclinB2 and Cdc2, but does not affect oocyte meiotic progression after GVBD

To further investigate the functions of PKCβ1 in meiotic maturation, exogenous Myc-PKCβ1 was overexpressed in mouse oocytes. We injected Myc or Myc-PKCβ1 mRNA (2.5mg/ml) into the GV oocytes, and incubated oocytes in M2 medium containing 200μm IBMX for 12h before collecting for Western blot analysis. As shown in Figure 8(a), we detected a band about 89kDa in the Myc-PKCβ1 mRNA injection group (1.4 ± 0.0495 in the overexpression group, 0.00 in the control group), which indicated that Myc-PKCβ1 was successfully expressed in mouse oocytes. Next, we counted the number of GVBD oocytes at 1, 2, 3 and 4 h after the oocytes had been washed 3 times and transferred to IBMX-free M2 medium. As shown in Figure 8(b), GVBD percentage in the Myc-PKCβ1 mRNA injection group (11.28 ± 0.28% at 1h; 36.80 ± 6.83% at 2h; 58.99 ± 4.27% at 3h; 65.2 ± 1.97% at 4h, n = 136) were significantly lower than in the control group (28.34 ± 2.3% at 1h; 66.44 ± 4.86% at 2h; 95.3 ± 4.11% at 3h; 95.84 ± 1.8% at 4h, n = 153). These results indicate that PKCβ1-overexpressed oocytes had a reduced capacity for meiotic resumption. Next, we examined Cyclin B1, Cyclin B2 in PKCβ1-overexpression oocytes. In mouse oocytes, Cyclin B1 is the regulatory subunit of MPF, increases of which at the GV stage can activate Cdc2, and promote G2/M transition. Cyclin B1 level in the PKCβ1-overexpression group (0.21 ± 0.02) was notably reduced compared with that in the control

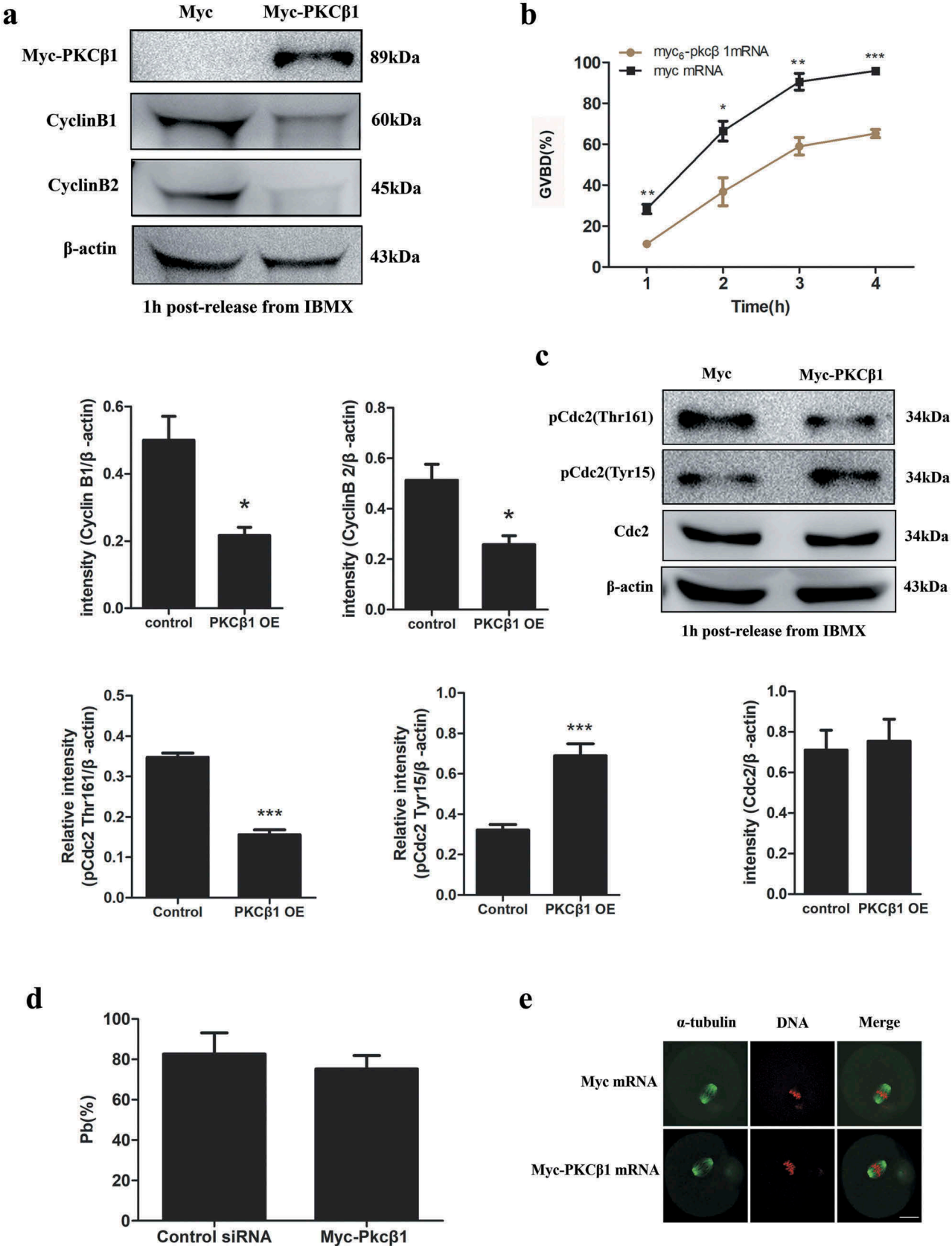
a
Myc
Myc-PKCβ1
Myc-PKCβ1
89kDa
CyclinB1
60kDa
CyclinB2
45kDa
β-actin
43kDa
1h post-release from IBMX
b
myc6-pkcβ 1mRNA
myc mRNA
GVBD(%)
Time(h)
c
Myc
Myc-PKCβ1
pCdc2(Thr161)
34kDa
pCdc2(Tyr15)
34kDa
Cdc2
34kDa
β-actin
43kDa
1h post-release from IBMX
intensity (Cyclin B1/β -actin)
control
PKCβ1 OE
intensity (CyclinB 2/β -actin)
control
PKCβ1 OE
Relative intensity (pCdc2 Thr161/β -actin)
Control
PKCβ1 OE
Relative intensity (pCdc2 Tyr15/β -actin)
Control
PKCβ1 OE
intensity (Cdc2/β -actin)
control
PKCβ1 OE
d
Pb(%)
Control siRNA
Myc-Pkcβ1
e
α-tubulin
DNA
Merge
Myc mRNA
Myc-PKCβ1 mRNA

group (0.50 ± 0.07, P < 0.05) (Figure 8(a)). The Cyclin B2 was also reduced significantly in the PKCβ1-overexpression group (0.25 ± 0.036) compared with that in the control group (0.51 ± 0.63, P < 0.05). We also examined Cdc2 activity by detecting its Thr161 and Tyr15 phosphorylation state. As shown in Figure 8(c), phosphorylation of the Thr161 of Cdc2, which is required for MPF activation, was decreased remarkably in the PKCβ1-overexpression group (0.12 ± 0.02) compared to that in the control group (0.34 ± 0.06, P < 0.001). Furthermore, higher level of Tyr15 of Cdc2 was detected in PKCβ1 overexpression group (0.689 ± 0.059) compared with that of the control group (0.32 ± 0.027, P < 0.001) by 1h following release from IBMX, suggesting that the dephosphorylation of the Tyr15 of Cdc2, which was required for MPF activation, was blocked. We found no significant change in Cdc2 at the protein level between the PKCβ1-overexpression group (0.71 ± 0.0179) and the control group (0.76 ± 0.0215, P > 0.05). All above suggested overexpression of PKCβ1 decreased MPF activity, and thus reduced the rate of GVBD.

For those oocytes which underwent GVBD after microinjection of myc or myc-PKCβ1 mRNA, they were further incubated for up to 14 h to observe PB1 extrusion. Myc-PKCβ1 mRNA injected oocytes showed no difference in the percentage of PB1 emission once GVBD occurred (Figure 8(d)). Immunostaining was performed to study the impact of myc-PKCβ1 mRNA injection on spindle morphology in these oocytes. The PKCβ1 mRNA injected oocytes displayed normal spindles (Figure 8(e)). One possibility was that overexpression of PKCβ1did not affect meiotic events after GVBD, and the other possibility was that the overexpression of PKCβ1 did not reach a threshold in these oocytes, which underwent GVBD at 2h.

Discussion

PKCβ1 is an important member of the family of conventional protein kinase C that play a crucial role in regulating the mitotic cell cycle [21,45]. Until now, the involvement of PKC in the regulation of meiosis has been studied by utilizing PKC activators or inhibitors, which are unable to discriminate between the different types of PKC [30,46]. In this study, we investigated the expression, localization and possible roles of PKCβ1 during mouse oocyte meiotic maturation. We found that p-PKCβ1, the active form of PKCβ1, displayed a clear cluster appearance at the spindle poles. Perturbation of PKCβ1 function using specific siRNA caused spindle assembly defects, and thus failure of meiotic metaphase-to-anaphase transition as well as homologous chromosome segregation. In turn, this caused failure of the first polar body extrusion. Furthermore, we showed that overexpression of PKCβ1 lead to maintenance of meiotic arrest by regulating Cdc2 and cyclin B. To our knowledge, this is the first study with RNAi and overexpression on the role of PKCβ1 during mouse oocyte meiotic maturation.

PKCβ1 was expressed in mouse oocytes from GV to MII stages, indicating the possible role of PKCβ1 in meiotic progression. As for mouse

Figure 8. Effects of PKCβ1 overexpression (OE) on oocyte meiotic maturation. (a) Western blotting of Myc-PKCβ1, Cyclin B1 and Cyclin B2 in myc or myc-PKCβ1 mRNA injected oocytes 1h following release form IBMX. The GV oocytes were microinjected with myc or myc-PKCβ1 mRNA, and incubated in M2 medium containing 200μm IBMX for 12h before being collected for Western blot analysis. The intensities of Cyclin B1/β-actin and Cyclin B2/β-actin were accessed by grey level analysis. Myc-PKCβ1 is 89kDa, CyclinB1 is 60kDa, CyclinB2 is 45kDa, β-actin is 43kDa. Each sample contained 200 oocytes. (b) Percentage of GVBD at 1, 2, 3 and 4h for myc or myc-PKCβ1 mRNA injected oocytes. After microinjection of myc or myc-PKCβ1 mRNA, oocytes were incubated in M2 medium containing 200μm IBMX for 12h, and then transferred to IBMX-free M2 medium to resume meiosis. Data are presented as means ± SEM of 3 independent experiments. (* p < 0.05, ** p < 0.01, *** p < 0.001). (c) The phosphorylation level of Tyr15 or Thr161 of Cdc2 and total Cdc2 in myc and myc-PKCβ1 mRNA injected oocytes 1h release form IBMX. The phosphorylation level of Tyr15 of Cdc2 increased, while the phosphorylation level of Thr161 of Cdc2 decreased in myc-PKCβ1 mRNA injected oocytes. The intensities of p-Cdc2 (Thr161)/β-actin, p-Cdc2(Tyr15)/β-actin and Cdc2/β-actin were accessed by grey level analysis. p-Cdc2 (Thr161) is 34kDa, p-Cdc2(Tyr15) is 34kDa, Cdc2 is 34kDa, β-actin is 43kDa. Each sample contains 200 oocytes. (*** p < 0.001) (d) Percentage of PBE at 14h for myc or myc-PKCβ1 mRNA injected GVBD oocytes. Oocytes were microinjected with myc or myc-PKCβ1 mRNA. The oocytes were incubated in M2 medium containing 200μm IBMX for 14h, and then transferred to IBMX-free M2 medium. The oocytes which underwent GVBD at 2h were further cultured up to 14 h to observe PBE. Data are presented as means ± SEM of 3 independent experiments. (e) Representative images of spindle and chromosomes in myc and myc-PKCβ1 mRNA injected oocytes. After microinjection of myc or myc-PKCβ1 mRNA, oocytes were incubated in M2 medium containing 200μm IBMX for 12h, and then transferred to IBMX-free M2 medium. The oocytes which underwent GVBD at 2h were further cultured up to 14h, followed by immunostaining with α-tubulin and Hoechst 33,342. Green, PKCβ1; red, chromatin. Bar = 20μm.

oocytes, contradictory findings have been reported concerning the nuclear localization of PKCβ1. Some authors have reported PKCβ1 presence in the cytoplasm before meiosis resumption, and it migrated to the germinal vesicle before GVBD [38], or exclusively in the cytoplasm in GV oocytes [29]. By both antibody staining and myc6-tagged-mRNA microinjection, we find that PKCβ1 mainly concentrated in the germinal vesicle with a weak expression in the cytoplasm, but evenly distributed in the cytoplasm and in the plasma membrane from pro-MI to MII stages, while it was located at the midbody at the telophase I stage.

Furthermore, we first showed that p-PKCβ1 concentrated at the spindle poles at metaphase, and faint p-PKCβ1 signals were detected at midbody in Anaphase I stage, very similar to several proteins, such as Nek9, Kif2a, p38α-MAPK, that we previously demonstrated to be needed for spindle assembly in oocyte maturation [47–49] . This localization pattern suggests that PKCβ1 may play important roles at different stages of mouse oocyte meiotic maturation.

In the present study, to dissect the role of PKCβ1 in mouse oocyte maturation, we knocked down PKCβ1 by siRNA microinjection. Immunoblot analysis confirmed that the PKCβ1 level was significantly reduced after siRNA injection. Knockdown of PKCβ1 resulted in severely reduced polar body extrusion. Spindles were disrupted and chromosomes were misaligned in some of the MI arrested oocytes, suggesting potentially abnormal spindle assembly (Figure 4). We did not observe any defects of spindle assembly and polar body extrusion in the PKCβ1 overexpression oocytes (Figure 8). The detailed mechanisms by which PKCβ1 regulates spindle assembly remain far from understood. Several lines of evidence implicate PKC function in regulating microtubule organization. First, the presence of p-PKCβ1 in meiotic spindle poles and in the central portion of the elongating meiotic spindle suggests that PKCβ1 activation might play a role in spindle organization as well as cytokinesis during mouse oocyte meiosis (Figure 3(c)). Secondly, a number of microtubule-associated proteins are substrates for PKC both in vitro and in vivo [38,50,51]. Thirdly, PKC agonists at very low concentrations can significantly promote the disassembly of spindle microtubules in mouse oocytes at the MI and MII stages [23,42,52]. Furthermore, there is evidence that phosphorylation of tubulin and microtubule-associated proteins contributes significantly to microtubule stability [41]. It has been established that PKCβI co-localizes with microtubules and bind microtubule-associated proteins, depletion of which resulted in defective microtubule reorganization in U937 leukemia cells [42] . Importantly, PKCβI-deficient T cells failed to develop a polarized microtubule network, a defect that can be rescued by expressing PKCβI [41] . Thus, PKC is emerging as a key regulator of microtubule organization both in mitosis and meiosis. It could be inferred that PKCβ1 through regulating microtubule function, or phosphorylation of tubulin associated proteins, is involved in meiotic spindle assembly. It would be interesting to determine which tubulin associated proteins are associated with PKCβ1 to control spindle microtubule organization.

SAC proteins including mitotic arrest-deficient-1 (Mad1), Mad2, budding uninhibited by benzimidazole-1 (Bub1), Bub3, BubR1 and monopolar spindle 1 (Mps1) proteins play critical roles in supervising proper chromosome segregation [53,54]. Knockdown of PKCβ1 caused significantly abnormal spindle assembly, chromosome misalignment and failed PB1 extrusion, indicating the possible activation of SAC. PKCβ1-knockdown oocytes were arrested at Pro-MI/MI, and chromosomes were still in bivalent stage. All above prompted us to ask whether PKCβ1 depletion may affect SAC activity. In our study, Bub3 and Mad1 were detected at the kinetochores in Pro-MI/MI arrested oocytes in the PKCβ1 depletion oocytes, which indicates unsuccessful attachment of chromosomes to the microtubule with proper tension, thus activation of SAC.

Previous studies have shown that polar body emission requires a classical RhoA contractile ring and Cdc42-mediated membrane protrusion [43]. Recently it has been showed that disruption of Cdc42 in oocytes inhibited polar body emission, which is due to loss of actin cap formation and the defective contract ring [55]. PKCβ activates Rho and Cdc42 and increases the positive feedback that underlies the rapid amplification of Rho and Cdc42 during midzone formation to regulate polar body emission [44], implying an association between PKCβ1 and cytokinesis. In our study, PKCβI was

present in the midbody at Tel1, suggesting that it is a core midzone component that might play a role in cytokinesis during mouse oocyte meiosis. Time lapse microscopy revealed that PKCβI-depleted oocytes were arrested at the Pro-MI/MI stage, and they failed to emit the first polar body for many hours. In sharp contrast, most oocytes in the control group reached the MII stage and extruded PB1 by 12h. These data strongly suggest that PKCβI may inhibit meiotic maturation progression after GVBD through both regulating microtubule function and cytokinesis.

It has been reported that PKC activators inhibited spontaneous GVBD in denuded oocytes but stimulated the meiotic resumption in CEOs through mediation of cumulus cells [30]. To determine the mechanism by which PKC activity influences meiosis resumption it will be necessary to obtain an assessment of the specific PKC isoforms and potential target substrates that are expressed in mouse oocytes. According to a previous report, PKCβ1 may function as a cell cycle check point mediator during the late G1 phase and may regulate S phase entry in vascular smooth muscle cell proliferation [56]. Furthermore, PKCβ1 colocalized with lamin A/C on the nuclear envelope, suggesting that PKCβ1 may participate in the germinal vesicle breakdown in mouse oocytes [31]. There was evidence that cytoplasmic PKCβ1 lead to the maintenance of meiotic arrest, but the nuclear PKCβ1 was involved in the induction of meiosis resumption [38]. PKC-mediated meiotic arrest seems to occur through the maintenance of PKCβ1 in the cytoplasm [31]. Here, in the present study, by myc6-PKCβ1 mRNA microinjection, we overexpressed PKCβ1 in GV oocytes. More than 35% of PKCβ1 overexpression oocytes were not able to resume meiosis by 4h following release from IBMX, whereas more than 95% Myc-mRNA-injected oocytes resumed meiosis. These results have provided solid evidence indicating that PKCβ1 is involved in the maintenance of meiotic resumption. It was shown that the inhibition of PKCβ1 by its inhibitor G06976 and LY333531 could not induce oocyte maturation, indicating that the inhibition of PKCβ1 has no effect on meiosis resumption [39]. Similar to these reports, we observed that depletion of PKCβ1 by its specific siRNA microinjection did not affect oocyte meiotic resumption.

It is well known that MPF, a complex of the catalytic subunit cyclin-dependent kinase (Cdk1, also known as Cdc2) and regulatory subunit cyclin B [57], remains inactive until Cdk1 is phosphorylated at Thr161 by Cdk inactivating kinase (CAK) and de-phosphorylated by Cdc25c at Thr14/Tyr15 [8,58]. The cyclin B family includes cyclinB1 and cyclin B2. Increased expression of cyclin B at the GV stage can activate CDK1 by altering its phosphorylation status, and promote oocyte meiotic resumption [59], the APC-Cdh1 mediated destruction of which is indispensable for preventing MPF activation during G2 arrest [60,61]. It has been established that PKC suppresses MPF activation through the induction of the cyclin-dependent kinase inhibitor p21 $^{waf1/cip1}$, which blocks Cdc2 activity, or through the down-regulation of phosphatase Cdc25 (thus inhibiting Cdc2 dephosphorylation) [25,26]. Consequently, alterations in cyclin B1 level and/or Cdc2 activity characterize many conditions that perturb meiotic resumption [14,60]. Our results showed that overexpression of PKCβ1 induced downregulation of CyclinB1 and CyclinB2. We also found that Thr161 of Cdc2 in PKCβ1 overexpression oocytes could not be phosphorylated and Tyr15 could not be de-phosphorylated, while there was no change in total Cdc2 at protein level. This indicates that the PKCβ1-dependent inhibition of cyclin B1 expression level and Cdc2 activity are important for the control of G2/M transition in mouse oocytes. Considering that the exogenous protein (myc6- PKCβ1) may fail to be expressed in a considerable number of oocytes, the difference of GVBD rates between the control group and the overexpression group might be more significant.

In conclusion, our data uncovered that PKCβ1 is an important regulator of oocyte meiotic maturation. PKCβ1 is required for regulating microtubule function and spindle organization, as well as cytokinesis during polar body emission. Additionally, by regulating CyclinB1, CyclinB2 and Cdc2, PKCβ1 may play an indispensable role in regulating MPF activity and prophase I arrest.

Materials and methods

Antibodies and reagents

Rabbit polyclonal anti-PKCβ1 antibody used for Western blotting and immunofluorescence was purchased from Santa Cruz Biotechnology (sc-209);

Rabbit polyclonal anti- p-PKCβ1 (phosphor T642) antibody for Western blotting and immune fluorescence was from Abcam (ab75657); mouse monoclonal anti-α-tubulin-FITC antibody was obtained from Sigma (76074); mouse monoclonal anti-Myc-FITC antibody was produced by Invitrogen (Catalog #: R953-25); rabbit polyclonal anti-bub3 antibody was purchased from Santa Cruz Biotechnology (sc-28258); mouse monoclonal anti-Mad1 antibody was from Santa Cruz Biotechnology (sc-137025); Mouse monoclonal anti-β-actin antibody was obtained from Santa Cruz Biotechnology (SC-8432); mouse monoclonal anti-cyclin B1 (Abcam,1:500); mouse monoclonal anti-Cyclin B2 antibody was from Abcam (ab18250); mouse monoclonal anti-Cdc2(Cdk1) antibody was from Abcam (ab18); rabbit anti-phospho-Cdc2(Cdk1)-Tyr15 phosphorylated antibody was from ABclonal (AP0016); rabbit polyclonal anti-Cdc 2(Cdk1) P34 (Thr161) antibody was from Santa Cruz (sc101654). Alexa Fluor@ 488-conjugate Goat anti-Rabbit IgG (H + L) and Alexa Fluor @594-conjugate Goat anti-Rabbit IgG (H + L) were produced by Termo Fisher Scientific (Catalog# A-11008, Catalog# A-11012); TRITC-conjugated goat anti-mouse IgG(H*L) was produced by Jackson ImmunoResearch Laboratories, Inc. and subpackaged by Zhongshan Golden Bridge Biotechnology Co. LTD (Cat#Zf-0313).

All chemicals and culture media were purchased from Sigma Chemical Company (St. Louis, MO, USA) unless noted otherwise.

Oocyte collection and culture

Animal care and handling of female ICR mice (6 to 8 wk old) were conducted in accordance with the guidelines from Animal Research Committee policies of the Institute of Zoology, Chinese Academy of Sciences. Immature oocytes with intact germinal vesicles were collected from ovaries and cultured in M2 medium under paraffin oil in 5% CO_2 in air. The oocytes were maintained at the GV stage in M2 medium with 200μm IBMX. For in vitro maturation, GV oocytes were washed thoroughly and cultured in M2 for 0h, 4h, 8h,10h,12h, corresponding to GV, GVBD, MI, TI or MII stages.

Construction of plasmids for PKcβ1 and m-RNA synthesis

Total RNA was extracted from 200 GV stage mouse oocytes with the RNeasy micro purification kit (Qiagen), and the first strand cDNA was generated with oligo(dT) primers, using an M-MLV first strand c DNA synthesis kit (Takara). The nested PCR was used to amplify the full length PKCβ1 with the following primers: F1: TCAGGCCGGCCGATGGCTGACCCGGCTGC-G, R1: GCTCTAGATTAGCTCTTGAC TTCAG GTTTTAA. The PCR products were purified and digested using XbaI and FSeI (New England Biolabs, Inc) and linked with Pcs2+ vector, in which the PKCβ1 sequence was linked to six Myc tags at its N-terminus. The PKCβ1- Pcs2+ vector was linearized by NdeI and then purified. Synthesis of capped mRNAs was produced by SP6 m MESSAGE m machine (Ambion) and then tailed with poly(A) polymerase Tailing kit (Epicenter, ap-31220). Finally, the mRNA was purified by RNeasy cleanup kit (QIAGEN). The concentration of mRNA was detected by a BECKMAN du530 Analyzer, and diluted to a concentration of 0.4 mg/ml for localization and 2.5 mg/ml for overexpression.

Real time quantitative PCR analysis

Each sample contained 50 oocytes, total RNA was extracted by using an RNeasy micro purification kit (Qiagen, Austin, TX, USA). Then, cDNA synthesis kit (Takara, Otsu, Japan) was employed to generated single-strand cDNA. The primers used for the amplification of PKCβ1 fragment are listed as follows. Forward: 5′-GTGTCAAGTCTGCTGCTTTGT-3′; Reverse: 5′- GTAGGACTGGAGTACGTGTGG-3′. Gapdh was chosen as the reference gene. The primers used for the amplification of Gapdh fragment are listed as follows. Forward: 5′-CCCC AATTGTGTCCGTCGTG-3′; Reverse: 5′-TGCCTGCTTCACCACCTTCT-3′. We utilized the Roche Light Cycler 480 to perform the PCR. Relative gene expression was measured with real-time quantitative PCR and the 2 (Delta Delta C(T)) method.

Microinjection of Myc-PKCβ1 mRNA or PKCβ1 siRNA and coinjection of β5-tubulin-GFP mRNA, H2B-RFP mRNA with PKCβ1 siRNAs or control siRNA

Microinjection was performed with Narishige microinjector and completely finished in 30 minutes. siRNAs were chemically synthesized by Gene Pharma. The sequences of PKCβ1 siRNAs were: PKCβ1 siRNA-1:5′- GCAGGGAUUCCAG UGUCAATT –3′; PKCβ1 siRNA-2:5′- GCUGCU GUAUGGACUUA UUTT –3′. The concentration of each siRNA was 30 μM. The same amount of scrambled siRNAs was used as control. Each oocyte received about 10 pl PKCβ1 siRNA or control siRNA.

To examine how PKCβ1 depletion disrupted the oocyte meiotic division process, we co-injected β5-tubulin-GFP mRNA and H2B-RFP mRNA synthesized in references 62 and 63 [62,63], with PKCβ1 siRNA or control siRNA into GV oocytes. Each oocyte received about 10 pl β5-tubulin-GFP mRNA, H2β-RFP mRNA and PKCβ1 siRNA or control siRNA. Oocytes were kept at the GV stage in IBMX-containing M2 medium for 24h.

For Myc-PKCβ1 expression, concentration of mRNA was 0.4 mg/ml (or 2.5 mg/ml for overexpression). Oocytes were kept at the GV stage in M2 medium containing IBMX for 12h.

Western blotting

A total of 200 oocytes at the appropriate stage of meiotic maturation were collected in SDS loading buffer and boiled for 5 min. Then proteins were separated in 10% acrylamide gels containing 0.1% SDS and electrically transferred to polyvinylidene difluoride (PVDF) membranes. After 3 times of washing with TBST buffer, the membranes were blocked in TBST containing 1% BSA for 1 hour at room temperature. The membranes were then incubated overnight at 4°C with rabbit polyclonal anti-PKCβ1 antibody (1:100), rabbit polyclonal anti-p-PKCβ1 (1:1000), mouse monoclonal anti-β-actin antibody (1:2000), mouse monoclonal anti-Myc antibody (1:2000), mouse monoclonal anti-cyclin B1 (1:500), mouse monoclonal anti-cyclin B2 antibody (1:1000), mouse monoclonal anti-Cdc2 antibody(1:500), rabbit anti-phospho-Cdc2-Tyr15 phosphorylated antibody (1:1000), rabbit polyclonal anti-Cdc2 (Cdk1) p34 (Thr 161) (1:100) . The membranes were then washed 3 times in TBST, 10 minutes each, and incubated with horseradish peroxidase (HPR)-conjugated goat anti-rabbit IgG or HRP-conjugated goat anti-mouse IgG, for 2 hours at room temperature. Finally, after 3 times of washing with TBST, the membranes were processed with the enhanced chemiluminescence detection system (Bio-RAD, CA).

Immunofluorescence and confocal microscopy

Oocytes were fixed in 4% paraformaldehyde in PBS (PH 7.4) for 30 min and then permeabilized with 0.5% Triton X-100 for 20 min. After being blocked in 1% BSA-supplemented PBS at room temperature for 1h, oocytes were then incubated over night at 4°C with primary antibodies as follows: rabbit polyclonal anti-PKCβ1 antibody (1:50); rabbit polyclonal anti-p-PKCβ1 antibody (1:100); mouse monoclonal anti-α tubulin-FITC antibody (1:100); mouse monoclonal anti-Myc-FITC antibody (1:100); rabbit polyclonal anti-bub 3 antibody (1:50); mouse monoclonal anti-Mad1 antibody (1:50).

Three times of washing in washing buffer (0.1% Tween 20 and 0.01% Triton X-100 in PBS) were followed. The ooyctes were labeled with Fluor@488-conjugated Goat anti-Rabbit IgG, F594-conjugated Goat anti-Rabbit IgG and TRITC-conjugated goat anti-mouse IgG for 2h at room temperature. After three washes in washing buffer, DNA was stained with Hoechst 33342 for 20 min. Finally, the oocytes were mounted on glass slides with anti-fade mounting medium (DABCO) to retard photobleaching, and examined with a confocal laser-scanning microscope (Zeiss LSM 780, Germany).

Chromosome spreading

Oocytes were exposed in Tyrode's solution (Sigma, T1788) at room temperature to remove the zona pellucida. After a brief recovery in M2 medium, oocytes were placed onto glass slides for breaking and fixing in a solution of 1% paraformaldehyde in distilled H_2O (pH 9.2) containing 0.15% Triton X-100 and 3mM dithiothreitol fresh methanol: glacial acetic acid (3:1). Finally, DNA on the slides was stained with 10μg/ml Hoechst 33,42 and

mounted for observation using a confocal laser-scanning microscope (Zeiss LSM 780, Germany).

Time-lapse live imaging experiments

Microtubule and chromosome dynamics were filmed on a Perkin Elmer precisely Ultra View Vox confocal imaging system. A narrow band pass EGFP and RFP filter set and a 30% cut neutral density filter from chroma were used. Exposure time was set ranging from 300-700ms depending on the tubulin-GFP and DNA-RFP fluorescence level. The acquisition of digital time-lapse image was controlled by IPlab (Scanalytics) or AQM6 (Andorl kinetic-imaging) software packages. Confocal images of spindles and chromosomes in live oocytes were acquired with a 10× oil objective on a spinning disk confocal microscope (Perkin Elmer).

Statistical analysis

For all experiments, at least three replications were performed. The number of oocytes observed (n) are given in parentheses. Data are expressed as means±s.e.m and analyzed with Student's t-test with SPSS13.0 software (SPSS Inc.). $P < 0.05$ was considered statistically significant.

Disclosure statement

No potential conflict of interest was reported by the authors.

Funding

This work was supported by the National Natural Science Foundation of China (31530049), The Research Team of Female Reproductive Health and Fertility Preservation (SZSM201612065), and Project for Medical Discipline Advancement of Health and Family Planning commission of Shenzhen Municipality (SZXJ2017003).

Author contributions

Zi-Yun Yi designed and conceived the experiments; Zi-Yun Yi wrote and all authors reviewed the manuscript. Wei-Ping Qian, Qing-Yuan Sun and Jie Qiao provided professional advice on experimental design and paper writing. Heide Schatten edited the manuscript. Qiu-Xia Liang, Tie-Gang Meng, Jian Li, Ming-Zhe Dong, Yi Hou, Ying-Chun Ouyang, Chun-Hui Zhang provided assistance on experiment performance.

ORCID

Jie Qiao http://orcid.org/0000-0003-2126-1376

References

[1] Yuichi N, Teruko N, Tilly JL. Aged mouse ovaries possess rare premeiotic germ cells that can generate oocytes following transplantation into a young host environment. Aging (Albany NY). 2009;1(12):971–978.
[2] Niikura Y, Niikura T, Wang N, et al. Systemic signals in aged males exert potent rejuvenating effects on the ovarian follicle reserve in mammalian females. Aging (Albany NY). 2010;2(12):999.
[3] Chaigne A, Verlhac MH, Terret ME. Spindle positioning in mammalian oocytes. Exp Cell Res. 2012;318 (12):1442–1447.
[4] Masui Y, Clarke HJ. Oocyte maturation. Int Rev Cytol. 1979;57:185.
[5] Homer H, Gui L, Carroll J. A spindle assembly checkpoint protein functions in prophase I arrest and prometaphase progression. Science. 2009;326(5955):991–994.
[6] Adhikari D, Zheng W, Shen Y, et al. Cdk1, but not Cdk2, is the sole Cdk that is essential and sufficient to drive resumption of meiosis in mouse oocytes. Hum Mol Genet. 2012;21(11):2476.
[7] Dorée M, Hunt T. From Cdc2 to Cdk1: when did the cell cycle kinase join its cyclin partner? J Cell Sci. 2002;115(12):2461–2464.
[8] Pagliuca FW, Collins MO, Choudhary JS. Coordinating cell cycle progression via cyclin specificity. Cell Cycle. 2011;10(24):4195.
[9] Diril MK, Ratnacaram CK, Padmakumar VC, et al. Cyclin-dependent kinase 1 (Cdk1) is essential for cell division and suppression of DNA re-replication but not for liver regeneration. Proc Natl Acad Sci U S A. 2012;109(10):3826–3831.
[10] Smits VA, Klompmaker R, Vallenius T, et al. p21 inhibits Thr161 phosphorylation of Cdc2 to enforce the G2 DNA damage checkpoint. J Biol Chem. 2000;275(39):30638.
[11] Oh JS, Han SJ, Conti M. Wee1B, Myt1, and Cdc25 function in distinct compartments of the mouse oocyte to control meiotic resumption. J Cell Biol. 2010;188 (2):199–207.
[12] Branzei D, Foiani M. Regulation of DNA repair throughout the cell cycle. Nat Rev Mol Cell Biol. 2008;9(4):297–308.
[13] Reis A, Chang HY, Levasseur M, et al. APCcdh1 activity in mouse oocytes prevents entry into the first meiotic division. Nat Cell Biol. 2006;8(5):539–540.

[14] Holt JE, Tran SM, Stewart JL, et al. The APC/C activator FZR1 coordinates the timing of meiotic resumption during prophase I arrest in mammalian oocytes. Development. 2011;138(5):905–913.
[15] Ledan E, Polanski Z, Terret ME, et al. Meiotic maturation of the mouse oocyte requires an equilibrium between cyclin B synthesis and degradation. Dev Biol. 2001;232(2):400.
[16] Lu Q, Smith GD, Chen DY, et al. Phosphorylation of mitogen-activated protein kinase is regulated by protein kinase C, Cyclic 3′,5′-adenosine monophosphate, and protein phosphatase modulators during meiosis resumption in rat oocytes1. Biol Reprod. 2001;64 (5):1444–1450.
[17] Sole P, Motlik SJ. Prophase I arrest and progression to metaphase I in mouse oocytes: comparison of resumption of meiosis and recovery from G2-arrest in somatic cells. Mol Hum Reprod. 2010;16(9):654.
[18] Tripathi A, Kumar KV, Chaube SK. Meiotic cell cycle arrest in mammalian oocytes. J Cell Physiol. 2010;223 (3):592.
[19] Sun QY, Miao YH. Towards a new understanding on the regulation of mammalian oocyte meiosis resumption. Cell Cycle. 2009;8(17):2741–2747.
[20] Mellor H, Parker PJ. The extended protein kinase C superfamily. Biochem J. 1998;332(2):281.
[21] Poli A, Mongiorgi S, Cocco L, et al. Protein kinase C involvement in cell cycle modulation. Biochem Soc Trans. 2014;42(5):1471.
[22] Spruck CH, Miguel MPD, Ryan A, et al. Requirement of Cks2 for the first metaphase/anaphase transition of mammalian meiosis. Science. 2003;300(5619):647.
[23] Viveiros MM, O'Brien M, Eppig JJ. Protein kinase C activity regulates the onset of anaphase I in mouse oocytes1. Biol Reprod. 2004;71(5):1525–1532.
[24] Mccubrey JA, Steelman LS, Chappell WH, et al. Advances in targeting signal transduction pathways. Oncotarget. 2012;3(12):1505–1521.
[25] Lange L, Keppnerwitter S, Grigat J, et al. Combinatorial inhibition of Plk1 and PKCβ in cancer cells with different p53 status. Oncotarget. 2014;5(8):2263–2275.
[26] De VF, Riccardi M, Malanga D, et al. PKC-dependent phosphorylation of p27 at T198 contributes to p27 stabilization and cell cycle arrest. Cell Cycle. 2012;11 (8):1583–1592.
[27] Quan H, Fan H, Meng X, et al. Effects of PKC activation on the meiotic maturation, fertilization and early embryonic development of mouse oocytes. Zygote. 2003;11(4):329–337.
[28] Bornslaeger EA, Poueymirou WT, Mattei P, et al. Effects of protein kinase C activators on germinal vesicle breakdown and polar body emission of mouse oocytes. Exp Cell Res. 1986;165(2):507–517.
[29] Luria A, Tennenbaum T, Sun QY, et al. Differential localization of conventional protein kinase C isoforms during mouse oocyte development1. Biol Reprod. 2000;62(6):1564.
[30] Downs SM, Cottom J, Hunzicker-Dunn M. Protein kinase C and meiotic regulation in isolated mouse oocytes. Mol Reprod Dev. 2001;58(1):101.
[31] Denys A, Avazeri N, Lefèvre B. The PKC pathway and in particular its β1 isoform is clearly involved in meiotic arrest maintenance but poorly in FSH-induced meiosis resumption of the mouse cumulus cell enclosed oocyte. Mol Reprod Dev. 2007;74(12):1575.
[32] Carbone MC, Tatone C. Alterations in the protein kinase C signaling activated by a parthenogenetic agent in oocytes from reproductively old mice. Mol Reprod Dev. 2009;76(2):122–131.
[33] Fan HY, Tong C, Li MY, et al. Translocation of the classic protein kinase C isoforms in porcine oocytes: implications of protein kinase C involvement in the regulation of nuclear activity and cortical granule exocytosis. Exp Cell Res. 2002;277(2):183–191.
[34] Fan HY, Huo LJ, Chen DY, et al. Protein kinase C and mitogen-activated protein kinase cascade in mouse cumulus cells: cross talk and effect on meiotic resumption of oocyte. Biol Reprod. 2004;70(4):1178–1187.
[35] Zheng ZY, Li QZ, Chen DY, et al. Translocation of phospho-protein kinase Cs implies their roles in meiotic-spindle organization, polar-body emission and nuclear activity in mouse eggs. Reproduction. 2005;129(2):229–234.
[36] Viveiros MM, Hirao Y, Eppig JJ. Evidence that protein kinase C (PKC) participates in the meiosis I to meiosis II transition in mouse oocytes. Dev Biol. 2001;235 (2):330.
[37] Black JD. Protein kinase C-mediated regulation of the cell cycle. Front Biosci. 2000;5(1):D406.
[38] Avazeri N, Courtot AM, Lefevre B. Regulation of spontaneous meiosis resumption in mouse oocytes by various conventional PKC isozymes depends on cellular compartmentalization. J Cell Sci. 2004;117(Pt 21):4969.
[39] Wang J, Qian C, Zhou J, et al. Specific protein kinase C isoforms α And βI are involved in follicle-stimulating hormone-induced mouse follicle-enclosed oocytes meiotic resumption. Plos One. 2012;7(9):e45043.
[40] Houben F, Ramaekers FC, Snoeckx LH, et al. Role of nuclear lamina-cytoskeleton interactions in the maintenance of cellular strength. Biochim Biophys Acta. 2007;1773(5):675.
[41] Volkov Y, Long A, Mcgrath S, et al. Crucial importance of PKC-beta(I) in LFA-1-mediated locomotion of activated T cells. Nat Immunol. 2001;2(6):508–514.
[42] Kiley SC, Parker PJ. Differential localization of protein kinase C isozymes in U937 cells: evidence for distinct isozyme functions during monocyte differentiation. J Cell Sci. 1995;108(3):1003.
[43] Zhang X, Ma C, Miller AL, et al. Polar body emission requires a rhoA contractile ring and Cdc42-mediated membrane protrusion. Dev Cell. 2008;15(3):386.
[44] Holmes WR, Liao L, Bement W, et al. Modeling the roles of protein kinase Cβ and η in single-cell wound repair. Mol Biol Cell. 2015;26(22):4100–4108.

[45] Newton AC. Protein kinase C: poised to signal. Am J Phys Endocrinol Metab. 2010;298(3):E395.
[46] Tůmová L, Romar R, Petr J, et al. The effect of protein kinase C activator and nitric oxide donor on oocyte activation and cortical granule exocytosis in porcine eggs. Animal. 2013;7(2):279–286.
[47] Yi ZY, Ma XS, Liang QX, et al. Kif2a regulates spindle organization and cell cycle progression in meiotic oocytes. Sci Rep. 2016;6:38574.
[48] Yang SW, Gao C, Chen L, et al. Nek9 regulates spindle organization and cell cycle progression during mouse oocyte meiosis and its location in early embryo mitosis. Cell Cycle. 2012;11(23):4366.
[49] Ou XH, Li S, Xu BZ, et al. p38α MAPK is a MTOC-associated protein regulating spindle assembly, spindle length and accurate chromosome segregation during mouse oocyte meiotic maturation. Cell Cycle. 2010;9 (20):4130–4143.
[50] Correas I, Díaznido J, Avila J. Microtubule-associated protein tau is phosphorylated by protein kinase C on its tubulin binding domain. J Biol Chem. 1992;267 (22):15721–15728.
[51] Robinson PJ. The role of protein kinase C and its neuronal substrates dephosphin, B-50, and MARCKS in neurotransmitter release. Mol Neurobiol. 1991;5(2–4):87–130.
[52] De VJ, Kiley S, Garris T, et al. Phorbol ester treatment of U937 cells with altered protein kinase C content and distribution induces cell death rather than differentiation. Cell Growth Differ. 1995;6(4):371–382.
[53] Wei L, Liang XW, Zhang QH, et al. BubR1 is a spindle assembly checkpoint protein regulating meiotic cell cycle progression of mouse oocyte. Cell Cycle. 2010;9 (6):1112–1121.
[54] Althoff F, Karess RE, Lehner CF. Spindle checkpoint-independent inhibition of mitotic chromosome segregation by drosophila Mps1. Mol Biol Cell. 2012;23(12):2275.
[55] Wang ZB, Jiang ZZ, Zhang QH, et al. Specific deletion of Cdc42 does not affect meiotic spindle organization/migration and homologous chromosome segregation but disrupts polarity establishment and cytokinesis in mouse oocytes. Mol Biol Cell. 2013;24(24):3832.
[56] Yamamoto M, Acevedoduncan M, Chalfant CE, et al. The roles of protein kinase C beta I and beta II in vascular smooth muscle cell proliferation. Exp Cell Res. 1998;240(2):349–358.
[57] Jones KT. Turning it on and off: M-phase promoting factor during meiotic maturation and fertilization. Mol Hum Reprod. 2004;10(1):1–5.
[58] Gavet O, Pines J. Progressive activation of cyclinB1-Cdk1 coordinates entry to mitosis. Dev Cell. 2010;18(4):533.
[59] Malumbres M, Barbacid M. Mammalian cyclin-dependent kinases. Trends Biochem Sci. 2005;30(11):630–641.
[60] Marangos P, Carroll J. Securin regulates entry into M-phase by modulating the stability of cyclin B. Nat Cell Biol. 2008;10(4):445.
[61] Solc P, Saskova A, Baran V, et al. CDC25A phosphatase controls meiosis I progression in mouse oocytes. Dev Biol. 2008;317(1):260–269.
[62] Verlhac MH, Lefebvre C, Guillaud P, et al. Asymmetric division in mouse oocytes: with or without Mos. Curr Biol. 2000;10(20):1303–1306.
[63] Wang L, Wang ZB, Zhang X, et al. Brefeldin A disrupts asymmetric spindle positioning in mouse oocytes. Dev Biol. 2008;313(1):155–166.